


PERSPECTIVE

Open Access



Synthesis strategies and obstacles of lignocellulose-derived hard carbon anodes for sodium-ion batteries

Wenli Zhang^{1,2,3,4*} , Zongyi Huang^{1,2}, Husam N. Alshareef^{5*} and Xueqing Qiu^{1,2*}

Abstract

In this perspective, we present an overview of the research and advancement of lignocellulose-derived hard carbon anodes and their pivotal role in the commercialization of sodium-ion batteries. Hard carbon anodes, sourced from lignocellulosic biomasses, exhibit considerable promise due to their widespread availability, economical viability, and environmentally friendly attributes with zero carbon-dioxide emissions. Given the intricate compositions and composite nature of lignocellulosic materials, it becomes imperative to prioritize factors crucial for the fabrication of hard carbon anodes that exhibit enhanced sodium-ion storage capabilities. Thus, our study offers an extensive overview of the structure and performance nuances of hard carbon anodes derived from cellulose, hemicellulose, and lignin. Furthermore, it delves into the fundamental principles governing synthesis methodologies and confronts the challenges inherent in producing lignocellulose-derived hard carbon anodes tailored specifically for sodium-ion batteries.

Highlights

- Lignocellulose is a promising low-cost precursor for the hard carbon anodes in sodium-ion batteries.
- Chemical, crystalline, components, and multi-dimensional structures of lignocellulose influence the structure and performance of hard carbon anodes.
- Engineering methodologies tuning the microstructures of lignocellulose could change the intrinsic structure and performances of hard carbon anodes.
- New methods also need to consider the principles of green chemistry and sustainable development.

Keywords Lignocellulose, Hard carbon, Sodium-ion battery, Multi-dimensional structure

Communicated by Fengchang Wu.

*Correspondence:

Wenli Zhang
wlzhang@gdut.edu.cn; hiteur@163.com

Husam N. Alshareef
husam.alshareef@kaust.edu.sa

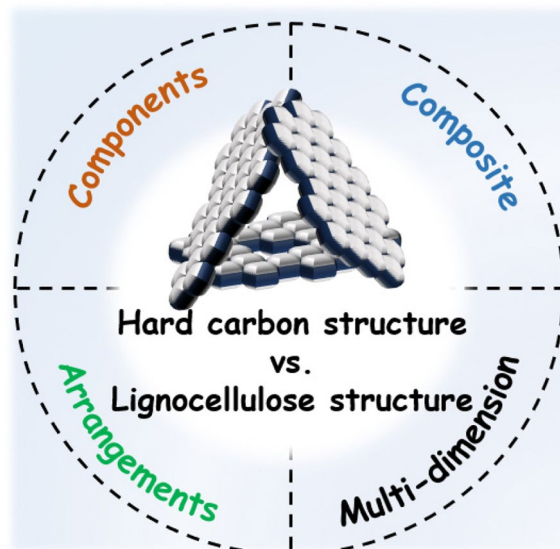
Xueqing Qiu
cexqqiu@scut.edu.cn

Full list of author information is available at the end of the article



© The Author(s) 2024. **Open Access** This article is licensed under a Creative Commons Attribution 4.0 International License, which permits use, sharing, adaptation, distribution and reproduction in any medium or format, as long as you give appropriate credit to the original author(s) and the source, provide a link to the Creative Commons licence, and indicate if changes were made. The images or other third party material in this article are included in the article's Creative Commons licence, unless indicated otherwise in a credit line to the material. If material is not included in the article's Creative Commons licence and your intended use is not permitted by statutory regulation or exceeds the permitted use, you will need to obtain permission directly from the copyright holder. To view a copy of this licence, visit <http://creativecommons.org/licenses/by/4.0/>.

Graphical Abstract



Sodium-ion battery (SIB) is currently a well-developed, next-generation commercial rechargeable battery technology (Usiskin et al. 2021). Given the abundant sodium resources in the earth's crust, SIB is deemed to be a cost-effective energy storage technology that could compete with the mature lead acid battery (LABs) (Yin et al. 2022) and lithium-ion battery (Xie and Lu 2020) technologies. Therefore, *the cost-effectiveness of the electrode materials and electrolytes should meet the low-cost design philosophy of SIBs*. Among the widely investigated anodes (conversion, alloy, intercalation, and carbonaceous) (Zhang et al. 2019) in research papers, hard carbon is the most practical, promising family of anodes for the commercialization of SIB due to its high capacity and low (de)sodiation potentials (Li et al. 2023). Moreover, hard carbons could be prepared from low-cost, abundant lignocellulose carbon precursors (Huang et al. 2023; Yang et al. 2023).

Hard carbon refers to the carbon materials obtained from resin, lignocellulose biomasses, and thermosetting plastics at moderate carbonization temperatures (1000 – 2000°C). These carbon materials can not be totally graphitized even under a high carbonization temperature of 2500°C. HC contains multi-dimensional structure aspects, such as micro graphite nanodomains (GND), defects, and close pores formed by the arrangements of these GNDs (Zhao et al. 2021). Therefore, the microcrystalline, closed pores, and defects in HC could influence its electrochemical sodium-ion storage behaviors. Basically, hard carbon stores sodium ions through an

“adsorption-intercalation-pore filling” mechanism (Sun et al. 2024). Under such a mechanism, *the development of HCs with high capacities should focus on aspects of high closed pore volume, while the development of high-rate HC should focus on aspects of abundant defects and large inter-layer spacing*.

Lignocellulose biomasses and their components (cellulose, hemicellulose, and lignin) are promising HC precursors that are available and abundant in the present papermaking and biorefinery factories (Zhang et al. 2022). Primary lignocellulose biomasses are coconut shells, rice husks, bamboo fibers, etc. These primary lignocellulose biomasses exhibit different physicochemical structures in terms of chemical structure (Meng et al. 2023), components, arrangements of constituents, composite, and multi-dimensional structures. *These multi-dimensional structure aspects could influence the pyrolysis and carbonization of lignocellulose so that the structure and electrochemical performances of hard carbon could also be influenced*. In this regard, research on the relationship between hard carbon structures and lignocellulose structure is important for developing HCs with high performances.

Understanding the single role of lignin, cellulose, and hemicellulose in the formation of hard carbon anodes is necessary since they not only have different chemical structures (Fig. 1) but also different aggregate states. Usually, lignin is of an amorphous 3D structure, and cellulose is composed of crystalline or amorphous regions.

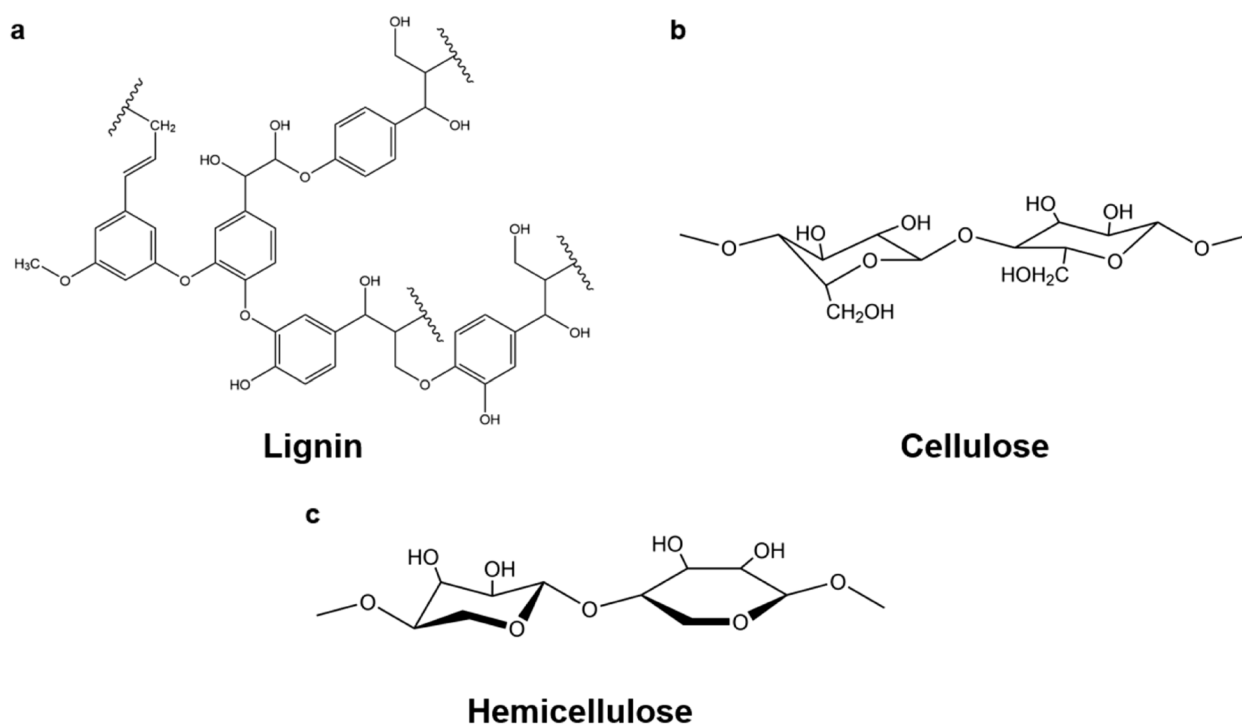


Fig. 1 The molecular structure of the precursors of HCs: (a) lignin, (b) cellulose, (c) hemicellulose

Hemicellulose is the binder between lignin and cellulose. In this perspective, we investigated the HCs derived from cellulose (not oxidized), lignin (enzymatic hydrolysis lignin), and hemicellulose (xylan) (denoted as CHC, LHC, and HCHC) under different calcination temperatures (600 – 1600°C) for 4 hours in nitrogen inert atmosphere with a heating ramping rate of 5 °C min⁻¹. Through powder X-ray diffraction (XRD) patterns of the HC samples, it is observed that CHC, LHC, and HCHC showed a similar tendency for the phenomenological (002) diffraction shapes until a carbonization temperature of 1600°C (Fig. 2a-c). At a carbonization temperature of 1600°C, LHC1600 displayed a small crystalline peak indicative of the formation of graphite microcrystalline. HCHC1600 showed a sharp diffraction peak suggesting the formation of larger graphite microcrystalline inside the carbon skeleton of HCHC1600. Some work reports the preferential formation of graphite crystalline in the cellulose-dominated biomass (Wang et al. 2021), which is ascribed to the existence of high content of cellulose component. Our results indicate that this preferential formation phenomenon is probably ascribed to the composite structure between cellulose and lignin/hemicellulose. Nevertheless, the formation of graphite nanodomains (GND) may influence the (002) interlayer spacing (d_{002}), the pore size, and the pore volume of closed pores.

It could be read from Fig. 2d that the d_{002} values of HCHC are relatively smaller (Tables 1, 2 and 3), which indicates the higher rate capabilities of LHC and CHCs compared with HCHC. The electrochemical performances of these HCs are compared in the following section.

Closed pores sizes and pore volumes determine the plateau capacities and rate capabilities, which are important parameters that influence the energy density of SIB full cells. Small-angle X-ray scattering (SAXS) techniques are usually used to determine the close pore size, pore volume, and pore size distribution (Fig. 3a-c). These pores are inaccessible to the electrolyte (Li et al. 2022; Chen et al. 2023), which allows a “pore-filling” charge storage mechanism. Pore size and pore volume should influence the sodium-ion storage performances (capacity and rate capabilities of the plateau and slope capacities). *Whether the pore size and crystalline structure could be changed during the sodium-ion storage process is a scientific issue.* The relationship between closed pores and plateau capacity is somewhat difficult to build since some of the pores are closed by GNDs which do not allow sodium ions to diffuse or intercalate. On the contrary, there are also open pores that do not allow electrolytes to go inside, which indicates that the pores are “closed” for the sodium-ion storage process. *The pore size could influence the formation of Na metal clusters, which determines the capacities*

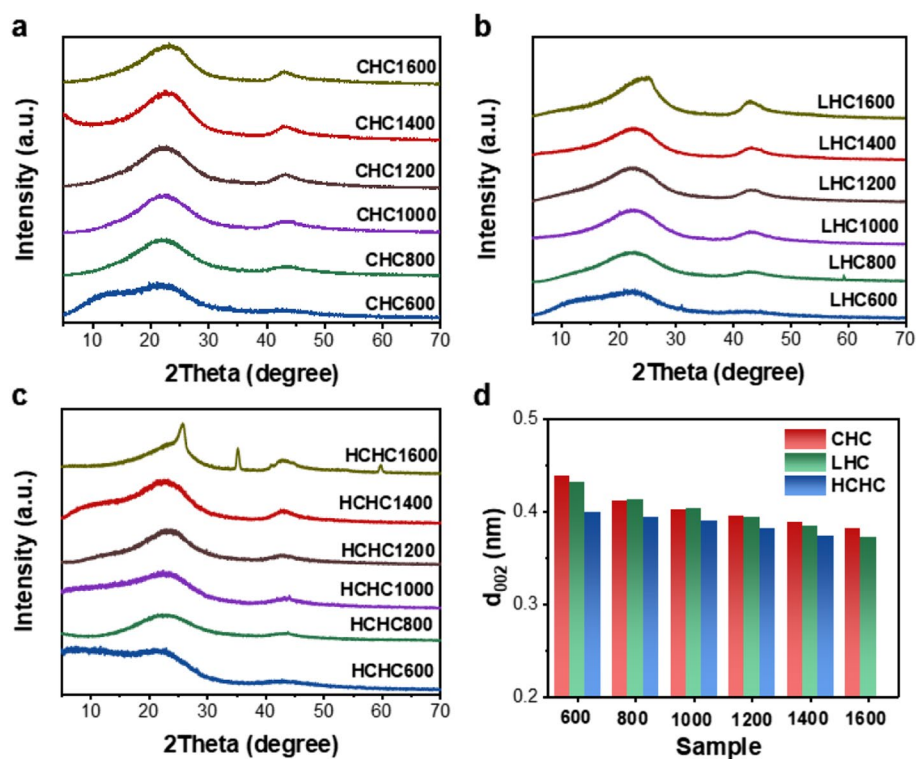


Fig. 2 Structural characterizations of HCs. **a** XRD patterns of CHCs. **b** XRD patterns of LHCs. **c** XRD patterns of HHCs. **d** The (002) interlayer spacing of CHCs, LHCs and HHCs

Table 1 Structure parameters of CHCs

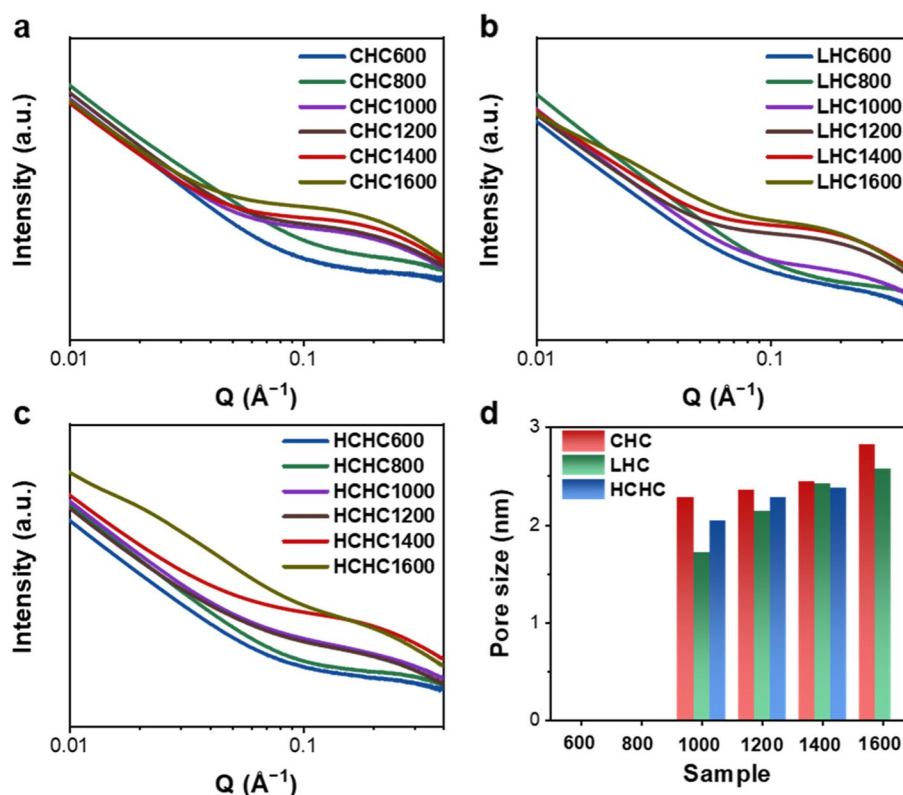
	2Theta (°)	FWHM (°)	D ₀₀₂ (nm)	L _a (nm)	L _c (nm)	n
CHC600	20.23	16.85	0.438	3.13	0.48	2.09
CHC800	21.58	11.71	0.411	3.32	0.69	2.68
CHC1000	22.08	10.16	0.402	3.59	0.80	2.99
CHC1200	22.52	10.47	0.395	3.90	0.78	2.97
CHC1400	22.89	8.74	0.388	4.30	0.93	3.39
CHC1600	23.27	9.67	0.382	3.62	0.84	3.20

Table 2 Structure parameters of LHCs

	2Theta (°)	FWHM (°)	D ₀₀₂ (nm)	L _a (nm)	L _c (nm)	n
LHC600	20.52	15.01	0.432	3.09	0.54	2.25
LHC800	21.54	11.06	0.412	3.60	0.73	2.77
LHC1000	22.01	10.23	0.404	4.13	0.79	2.95
LHC1200	22.61	10.28	0.392	4.05	0.79	3.01
LHC1400	23.16	10.34	0.384	4.58	0.82	3.14
LHC1600	23.88	9.96	0.372	4.48	0.81	3.18

Table 3 Structure parameters of HCHCs

	2Theta (°)	FWHM (°)	D ₀₀₂ (nm)	L _a (nm)	L _c (nm)	n
HCHC600	22.23	13.91	0.399	3.45	0.58	2.45
HCHC800	22.58	10.09	0.393	4.46	0.80	3.03
HCHC1000	22.69	9.91	0.391	3.85	0.82	3.09
HCHC1200	23.28	9.76	0.382	4.15	0.84	3.20
HCHC1400	23.80	8.04	0.374	3.97	1.01	3.71
HCHC1600	—	—	—	—	—	—

**Fig. 3** a SAXS patterns of CHCs. b SAXS patterns of LHCs. c SAXS patterns of HCHCs. d Dependence of closed pore size and closed pore volume (calculated from SAXS) on the carbonization temperatures of CHCs, LHCs and HCHCs

and rate capabilities of the plateau charge-discharge behaviors. The closed pore size of HCs is in the range of 1.5 to 3.0 nm (Fig. 3d). The closed pore size of CHC is larger than LHC and HCHC under the same calcination temperature, which needs to be explained in future research. A possible reason is that the thermal stability of hemicellulose is much inferior to cellulose and lignin, which induces extensive decomposition at low pyrolysis temperatures. The same tendency is found in lignin with different units (Yang et al. 2023). The larger closed pores of CHC could be due to the large GND formed from cellulose.

The galvanostatic charge-discharge (GCD) technique is used to test the electrochemical sodium-ion storage performances of HC anodes (Fig. 4). It is observed that the behaviors are similar for these HCs, which indicates that the intrinsic structures of HCs are similar. However, the capacities (including the plateau capacities) of LHC and CHC are much higher than HCHC, while they have similar initial coulombic efficiencies (ICEs). The result indicates that we could prepare hard carbons with higher capacities using lignocellulose with a low content of hemicellulose. The relatively low ICEs should be ascribed to the abundance of surface defects. Statistics results show

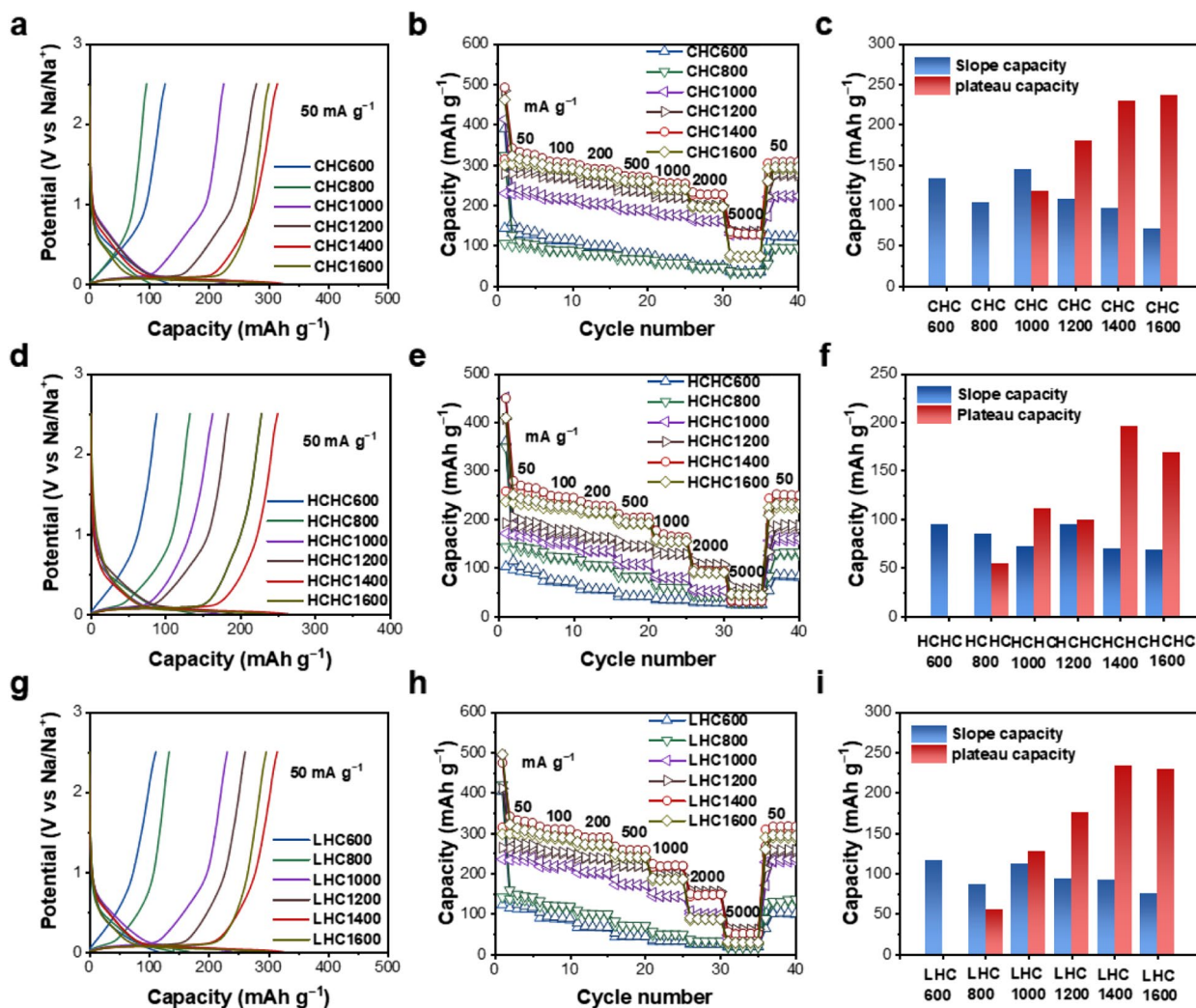


Fig. 4 Electrochemical performances of HCs. **a** GCD curve of CHCs. **b** Rate performances of CHCs. **c** The contributions of slope-region capacity (> 0.1 V) and plateau-region capacity (< 0.1 V) in the 5th discharge process of CHCs. **d** GCD curve of LHCs. **e** Rate performances of LHCs. **f** The contributions of slope-region capacity (> 0.1 V) and plateau-region capacity (< 0.1 V) in the 5th discharge process of LHCs. **g** GCD curve of HCHCs. **h** Rate performances of HCHCs. **i** The contributions of slope-region capacity (> 0.1 V) and plateau-region capacity (< 0.1 V) in the 5th discharge process of HCHCs

Table 4 Slope, plateau and reversible capacities of CHCs

	Slope capacity (mAh g ⁻¹)	Plateau capacity (mAh g ⁻¹)	Reversible capacity (mAh g ⁻¹)	ICE (%)
CHC600	133	0	133	36.7
CHC800	103	0	103	32.5
CHC1000	114	118	232	55.6
CHC1200	108	180	288	57.4
CHC1400	96	229	325	63.8
CHC1600	71	237	308	64.9

Table 5 Slope, plateau and reversible capacities of HCHCs

	Slope capacity (mAh g ⁻¹)	Plateau capacity (mAh g ⁻¹)	Reversible capacity (mAh g ⁻¹)	ICE (%)
HCHC600	95	0	95	28.5%
HCHC800	85	54	139	40.9%
HCHC1000	72	101	173	37.9%
HCHC1200	94	99	193	47.2%
HCHC1400	70	195	264	57.2%
HCHC1600	69	169	238	57.8%

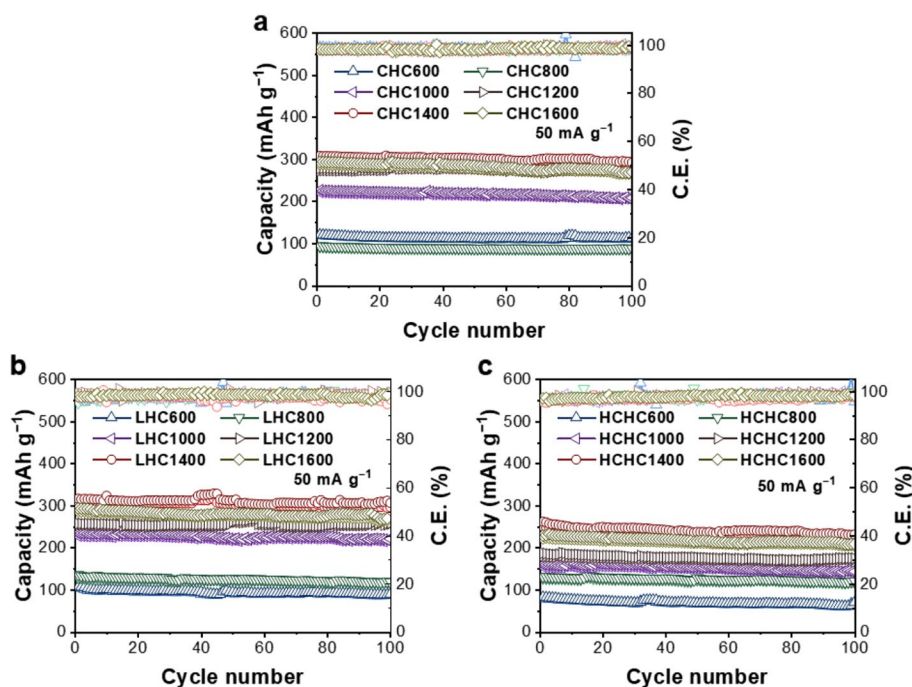
Table 6 Slope, plateau and reversible capacities of LHCs

	Slope capacity (mAh g ⁻¹)	Plateau capacity (mAh g ⁻¹)	Reversible capacity (mAh g ⁻¹)	ICE (%)
LHC600	116	0	116	30.3%
LHC800	86	55	141	33.7%
LHC1000	112	127	239	47.8%
LHC1200	94	176	270	64.3%
LHC1400	92	233	325	66.3%
LHC1600	75	230	305	60.2%

the plateau capacities and the slope capacities of these HCs (Fig. 4c, f, i), the plateau capacities of LHC and CHC are higher than that of HCHCs (Tables 4, 5 and 6), which is ascribed to the higher closed pore volume storing sodium metal cluster in this potential range. The closed pore volumes of most HCs are in the range of 0.2 to 0.3 cm³ g⁻¹ which gives rise to plateau capacities around 200 mAh g⁻¹ according to the full filling of these pores by Na clusters. *The closed pore volume could be tuned meticulously to meet the demand for developing HCs with higher plateau capacities.* A variety of pore engineering methods should be applied to the pyrolysis and carbonization of lignocellulose to achieve HCs with high capacities. HCs with stable GCD cycling stabilities coupled with stable cathodes should be employed to construct SIB full cells

with superior cycling stabilities. HCs show stable cycling stabilities under a GCD current density of 100 mA g⁻¹ (Fig. 5). However, it must be guaranteed that under high current densities, long cycling regimes, and extreme temperatures, the cycling stability of HCs is still superior to building stable SIBs. *The failure mode of HC should be investigated and improved to meet commercialization requirements.*

Given the abundant nature of lignocellulose biomasses on the earth, it is natural to develop low-cost HCs for commercial SIBs. The intrinsic pyrolysis and carbonization mechanism should be analyzed to track the formation mechanism of HCs derived from these single components and lignocellulose biomasses. Primary lignocellulose biomass is of particular interest since these raw materials of HCs are inexpensive and abundant in the Earth. However, firstly, *for developing commercial HCs, the consistency of lignocellulose biomasses must be guaranteed.* Consistency means that the composition, composite structure, and multi-dimension structures are reproducible. Secondly, *the electrochemical performances of HC could be tuned by chemical and chemical engineering methods.* In this regard, the extraction of chemicals could result in lignocellulose biomasses with changed structures and the tuning of the aggregate of lignocellulose. These aggregates could have different pyrolysis and carbonization behaviors, which could result in HCs with different structures (Tang et al. 2023). Therefore, *aggregate and structure regulation is*

**Fig. 5** a Cycling stability of CHCs at 50 mA g⁻¹. b Cycling stability of LHCs at 50 mA g⁻¹. c Cycling stability of HCHCs at 50 mA g⁻¹

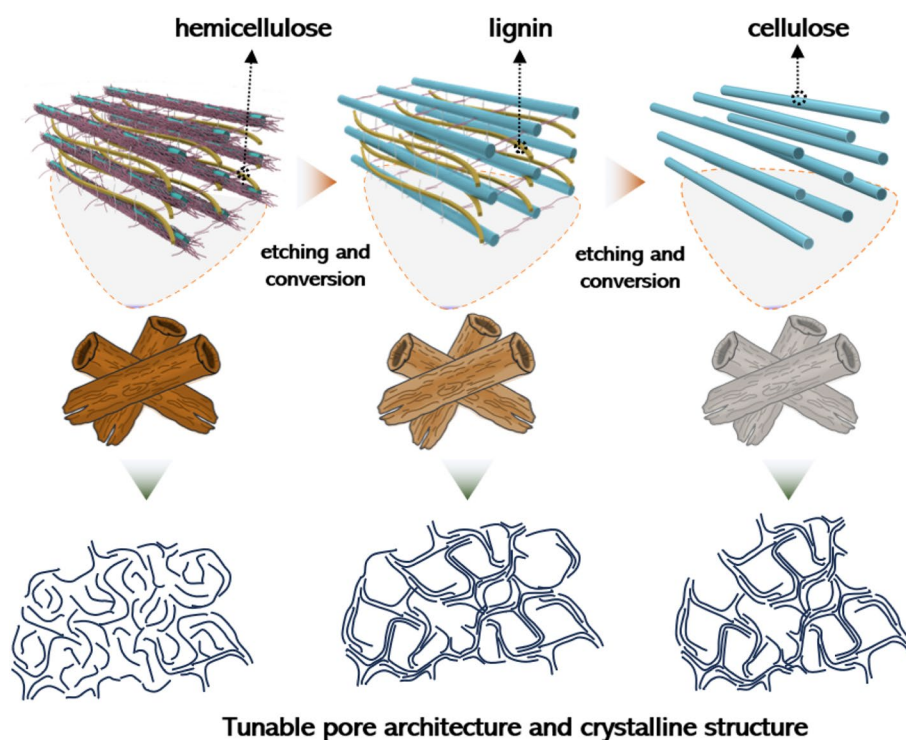


Fig. 6 Chemical structure tuning for the construction of lignocellulose with engineered multi-dimensional structures toward building HCs with different structures

an important strategy for constructing the lignocellulose precursors for HCs. Mature methods are built to separate hemicellulose, lignin, and cellulose sequentially (Fig. 6) using etching and conversion methods, such as dehydration, dissolution, oxidation, and lignin-first strategies. In such a way, the inconsistency of the raw materials should be tuned as raw materials for HC commercially employed in SIBs. Thirdly, these chemical processes should follow the principles of green chemistry and the ideas of sustainable development. In these chemical processes, less contaminant is released, and the components of the lignocellulose biomass should be fully utilized. To meet the huge demand for hard carbon anodes, lignocellulose should be produced in a large amount.

Abbreviations

SIB	Sodium-ion battery
LAB	Lead-acid battery
LIB	Lithium-ion battery
HC	hard carbon
CHC	cellulose-derived hard carbon
HCHC	hemicellulose-derived hard carbon
LHC	lignin-derived hard carbon
XRD	X-ray diffraction
SAXS	Small-angle X-ray scattering
ICE	initial coulombic efficiency
GCD	Galvanostatic charge-discharge

Acknowledgments

The authors acknowledge the financial support from the National Natural Science Foundation of China (U23A6005, 22108044), and the Research and Development Program in Key Fields of Guangdong Province (2020B1111380002). The authors acknowledge the financial support from the National Natural Science Foundation of China (U23A6005, 22108044), the Research and Development Program in Key Fields of Guangdong Province (2020B1111380002), the Open Foundation of Shanghai Jiao Tong University Shaoxing Research Institute of Renewable Energy and Molecular Engineering (JDSX2023002), and the user projects of Shanghai Synchrotron Radiation Facility (SSRF) (No. 2022-NFPS-PT-500103, 2023-NFPS-PT-500787, 2023-NFPS-JL-02050). We acknowledge the Analysis and Test Center, Guangdong University of Technology (GDUT) for the structural analysis (TEM, SEM, and Raman) of our specimens. We acknowledge the artwork (Fig. 6) drawn by Xiaoshan Zhang in our research group. The authors acknowledge the Analysis and Test Center, Guangdong University of Technology for the structural analysis of our specimens.

Authors' contributions

All authors contributed to the study conception and design. Writing review and editing, supervision, visualization, project administration, and funding acquisition were performed by Wenli Zhang and Xueqing Qiu. Data acquisition was prepared by Zongyi Huang. Writing review and editing were also performed by Husam N. Alshareef.

Funding

National Natural Science Foundation of China (U23A6005, 22108044), Research and Development Program in Key Fields of Guangdong Province (2020B1111380002), the Open Foundation of Shanghai Jiao Tong University Shaoxing Research Institute of Renewable Energy and Molecular Engineering (JDSX2023002), and the user projects of Shanghai Synchrotron Radiation Facility (SSRF) (No. 2022-NFPS-PT-500103, 2023-NFPS-PT-500787, 2023-NFPS-JL-02050).

Availability of data and materials

The research data reported in this work can be available upon reasonable request.

Declarations

Competing interests

The authors declare that they have no known competing financial interests or personal relationships that influence the work reported in this paper.

Author details

¹Guangdong Provincial Laboratory of Chemistry and Fine Chemical Engineering Jieyang Center, Jieyang 515200, China. ²School of Chemical Engineering and Light Industry, Guangdong University of Technology (GDUT), 100 Waihuan Xi Road, Panyu District, Guangzhou 510006, China. ³School of Advanced Manufacturing, Guangdong University of Technology (GDUT), Jieyang, Jieyang 522000, China. ⁴Shaoxing Research Institute of Renewable Energy and Molecular Engineering, Shanghai Jiao Tong University, Shaoxing 312000, China. ⁵Materials Science and Engineering, Physical Science and Engineering Division, King Abdullah University of Science and Technology (KAUST), 23955-6900 Thuwal, Saudi Arabia.

Received: 25 January 2024 Revised: 8 March 2024 Accepted: 15 March 2024

Published online: 26 March 2024

References

- Chen X, Sawut N, Chen K et al (2023) Filling carbon: a microstructure-engineered hard carbon for efficient alkali metal ion storage. *Energy Environ Sci* 16:4041–4053. <https://doi.org/10.1039/d3ee01154b>
- Huang S, Qiu X, Wang C et al (2023) Biomass-derived carbon anodes for sodium-ion batteries. *New Carbon Mater* 38:40–72. [https://doi.org/10.1016/S1872-5805\(23\)60718-8](https://doi.org/10.1016/S1872-5805(23)60718-8)
- Li Y, Vasileiadis A, Zhou Q et al (2023) Origin of fast charging in hard carbon anodes. *Nat Energy*. <https://doi.org/10.1038/s41560-024-01459-0>. <https://doi.org/10.1038/s41560-023-01414-5>
- Li Q, Liu X, Tao Y et al (2022) Sieving carbons promise practical anodes with extensible low-potential plateaus for sodium batteries. *Nat Sci Rev* 9:nwac084
- Meng Q, Chen B, Jian W et al (2023) Hard carbon anodes for sodium-ion batteries: Dependence of the microstructure and performance on the molecular structure of lignin. *J Power Sources* 581:233475. <https://doi.org/10.1016/j.jpowsour.2023.233475>
- Sun Y, Hou R, Xu S et al (2024) Molecular Engineering Enabling High Initial Coulombic Efficiency and Robust Solid Electrolyte Interphase for Hard Carbon in Sodium-Ion Batteries. *Angew Chemie Int Ed*. <https://doi.org/10.1002/anie.202318960>. <https://doi.org/10.1002/anie.202318960>
- Tang Z, Zhang R, Wang H et al (2023) Revealing the closed pore formation of waste wood-derived hard carbon for advanced sodium-ion battery. *Nat Commun* 14:6024. <https://doi.org/10.1038/s41467-023-39637-5>
- Usiskin R, Lu Y, Popovic J et al (2021) Fundamentals, status and promise of sodium-based batteries. *Nat Rev Mater* 12:1020–1035. <https://doi.org/10.1038/s41578-021-00324-w>
- Wang P, Zhang G, Wei XY et al (2021) Bioselective Synthesis of a Porous Carbon Collector for High-Performance Sodium-Metal Anodes. *J Am Chem Soc* 143:3280–3283. <https://doi.org/10.1021/jacs.0c12098>
- Xie J, Lu YC (2020) A retrospective on lithium-ion batteries. *Nat Commun* 11:2499
- Yang S, Zhang Z, Qiu X et al (2023) Engineering of the microstructures of enzymatic hydrolysis lignin-derived hard carbon anodes for sodium-ion batteries. *Resour Chem Mater* 2:245–251. <https://doi.org/10.1016/j.recmm.2023.06.001>
- Yin J, Lin H, Shi J et al (2022) Lead-carbon batteries toward future energy storage: from mechanism and materials to applications. *Electrochem Energy Rev* 5:2. <https://doi.org/10.1007/s41918-022-00134-w>
- Zhang W, Zhang F, Ming F, Alshareef HN (2019) Sodium-ion battery anodes: status and future trends. *EnergyChem* 1:100012. <https://doi.org/10.1016/j.enchem.2019.100012>

Zhang W, Qiu X, Wang C et al (2022) Lignin derived carbon materials: current status and future trends. *Carbon Res* 1:14. <https://doi.org/10.1007/s44246-022-00009-1>

Zhao LF, Hu Z, Lai WH et al (2021) Hard Carbon Anodes: Fundamental Understanding and Commercial Perspectives for Na-Ion Batteries beyond Li-Ion and K-Ion Counterparts. *Adv Energy Mater* 11:2002704. <https://doi.org/10.1002/aenm.202002704>

Publisher's Note

Springer Nature remains neutral with regard to jurisdictional claims in published maps and institutional affiliations.